https://doi.org/10.5194/tc-2021-155
Preprint. Discussion started: 15 June 2021

The Cryosphere Discussions
Open Access
EGU

Modelling the mass budget and future evolution of Tunabreen, central Spitsbergen

Johannes Oerlemans[1], Jack Kohler[2], Adrian Luckman[3]

[1]Institute for Marine and Atmospheric Research, Utrecht University, Princetonplein 5, Utrecht, 3585CC, The Netherlands
[2]Norsk Polarinstitutt, Hjalmar Johansengate 14, Trømso, Norway 9296
[3]Department of Geography, Swansea University, Singleton Park. Swansea, SA2 8PP, United Kingdom

Correspondence to: Johannes Oerlemans (j.oerlemans@uu.nl)

Abstract. Tunabreen is a 26-km long tidewater glacier. It is the most frequently surging glacier in Svalbard, with four documented surges in the past hundred years. We have modelled the evolution of this glacier with a Minimal Glacier Model (MGM), in which ice mechanics, calving and surging are parameterized. The model geometry consists of a flow band to which three tributaries supply mass. The calving rate is set to the mean observed value for the period 2012-2019, and kept constant. For the past 120 years, a smooth Equilibrium Line Altitude (ELA) history is reconstructed by finding the best possible match between observed and simulated glacier length. There is a modest correlation between this ELA history and meteorological observations from Longyearbyen.

The simulated glacier retreat is in good agreement with observations. Runs with and without surging show that the effect of surging on the long term glacier evolution is limited. Due to the low surface slope and associated strong height -mass balance feedback, Tunabreen is very sensitive to changes in ELA. For a constant future ELA equal to the reconstructed value for 2020, the glacier front will retreat by 8 km during the coming hundred years. For an increase of the ELA of 2 m per year, the retreat is projected to be 13 km and Tunabreen becomes a land-based glacier around 2100.

The calving rate is an important parameter: increasing its value by 50 % has about the same effect as a 50 m increase in the ELA, the corresponding equilibrium glacier length being 18 km (as compared to 25.8 km in the reference state).

Response times vary from 150 to 400 years, depending on the forcing and on the state of the glacier (tidewater or land-based).

1 Introduction

Tunabreen is a 26-km long tidewater glacier in central Spitsbergen (Figure 1). It is the most frequently surging glacier in Svalbard, with four documented surges during the past hundred years (Flink et al., 2015; Luckman et al., 2015). The surges occurred during 1924-1930 (advance 3 km), 1966-1971 (advance 2.1 km), 2002-2004 (advance 2 km), and 2016-2018 (advance 1.1 km). It appears that the frequency of surging has been increasing, with shorter duration of the periods of advance (Figure 2). Analysis of crevasse patterns visible on high-resolution satellite images has shown that surging is initiated close to the glacier front and then propagates upward (Flink et al., 2015).

Apart from the length fluctuations related to the surges, over the past hundred years Tunabreen has become shorter by about 1.5 km. This is likely due to an increasing Equilibrium Line Altitude (ELA) caused by rising air temperature (Førland et al., 2011), perhaps in combination with larger calving rates associated with higher ocean temperature (Luckman et al., 2015).

https://doi.org/10.5194/tc-2021-155
Preprint. Discussion started: 15 June 2021

The Cryosphere Discussions
Open Access
EGU

Before 1920 the lower parts of Tunabreen and of Von Postbreen were joined to form one front in the Tempelfjorden. Length data back to 1870 exist (Flink et al., 2015), but are not considered here for model validation because the focus is on the period that Tunabreen was an independently calving glacier.

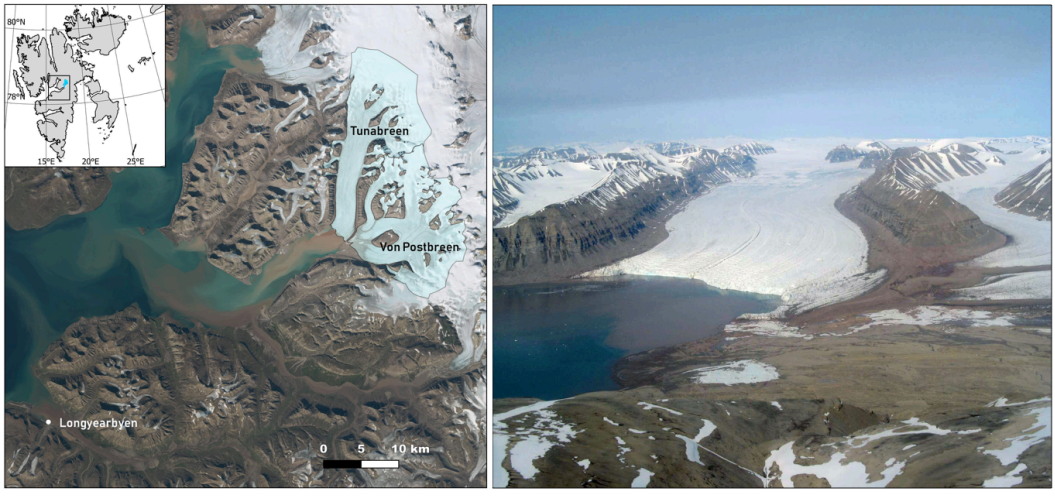

Figure 1. Left: Location of Tunabreen and von Postbreen in Svalbard (inset). Background image is from a 2020 Sentinel-2 mosaic (https://toposvalbard.npolar.no). Right: Photograph of Tunabreen in 2015 (© Anders Skoglund, Norwegian Polar Institute).

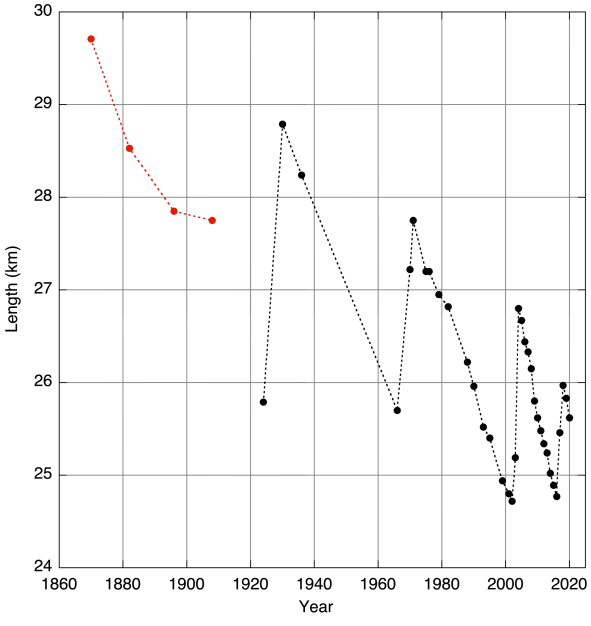

Figure 2. Length of Tunabreen from historical documents, aerial photographs and satellite images (Flink et al. 2015, with additions). The first four data points in red refer to the period that Tunabreen and Von Postbreen formed a joined front.

https://doi.org/10.5194/tc-2021-155
Preprint. Discussion started: 15 June 2021

The goal of this study is to analyse the mass budget of Tunabreen, to determine how sensitive the glacier is to ongoing and future climate warming, and to see if the frequent surging has an effect on its long-term retreat.

The model we used is a so-called Minimal Glacier Model (MGM, Oerlemans 2011), in which dynamic processes are parameterized. In this class of models, ice mechanics are not explicitly considered, but a number of essential feedback mechanisms can be dealt with (height - mass balance feedback, effect of reversed bed slopes, variable calving rates, effect of regular surging on the long-term mass budget, inclusion of tributary glaciers and basins). The basic idea behind a MGM is that, with respect to long-term evolution of glaciers, ice mechanics are 'slaved' by the exchange of mass with the environment (atmosphere and ocean). However, the most important mechanical effect, namely that glaciers are thicker when they are longer and/or rest on a bed with a smaller slope, should always be accounted for. We note that the model version employed here is similar to the one used in a study of Monacobreen in northern Spitsbergen (Oerlemans, 2018).

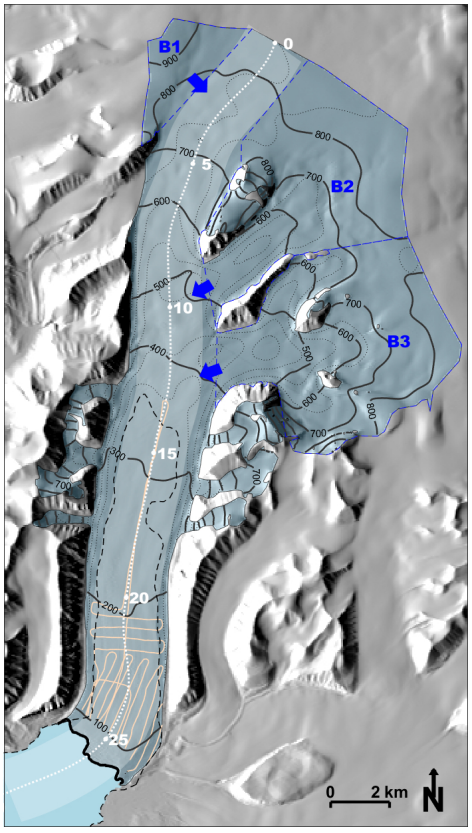

Figure 3. Map of Tunabreen. Surface contours (thick black lines) at 100-m intervals are from the NPI S0 DEM (Norwegian Polar Institute, 2014), based on aerial photography from 2009 (lower glacier tongue, 0-450 masl) and 2011 (upper glacier, > 450 masl). Bed contours (dotted black lines) at 100-m intervals are based on the Fürst et al (2018) reconstruction in the upper glacier, and 2015 helicopter radar (K. Lindback & J. Kohler, in Welty et al 2020) measurements (peach lines) in the lower glacier. Dashed subglacial contour shows the part of the bed below sea level. Center line profile (dotted white line) along 2200-m wide main flow band (lighter blue) shows distance from the ice divide at 5-km intervals. Three upper basins (blue dashed outlines) supply mass to the main flow band (blue arrows).

https://doi.org/10.5194/tc-2021-155
Preprint. Discussion started: 15 June 2021


The Cryosphere Discussions
Open Access
EGU

2 Glacier model

Tunabreen is modelled as a stream (flowband) of length L and constant width W. Three tributary glaciers / basins supply mass to the main stream if they have a positive mass budget (Figure 3). A few minor tributaries are neglected because they have no significant effect on the total mass budget of Tunabreen. The x-axis, originating at the ice divide, follows the centre line of the flow band. L is measured along this axis. Defined in this way, the glacier stand in 2009 serves as a reference point with L = 25.8 km. The average width of the flow band is taken as 2200 m.

Conservation of mass (or volume, since ice density is considered to be constant) determines the evolution of the glacier. It can be formulated as:

$$\frac{dV}{dt} = F + M_m + \sum_{i=1}^{3} M_i = M_{tot} \, . \tag{1}$$

Here V is the volume of the main stream of Tunabreen, F is the calving flux (< 0), M is the surface mass budget of the main stream, and the M_i are the contributions from the tributary glaciers. In the following sections a number of parameterizations are introduced concerning the global ice mechanics, geometry, calving, and climate forcing.

We stress that a Minimal Glacier Model is fundamentally different from another class of approximate models that have become popular, so called lumped-parameter models (e.g. Fowler et al., 2001; Benn et al. 2019). In the MGM the basic idea is to have a model description that deals with the conservation laws integrated over an entire glacier. This is essential if one wants to compute the evolution of a glacier for imposed environmental change. In the lumped-parameter model the focus is more on the details of local mechanical processes and their interaction with hydrology and thermodynamics - the large-scale glacier parameters are then specified.

2.1 Prognostic equation for glacier length

The glacier volume V (of the main stream) is given by WLH_m , where H_m is the mean ice thickness. Differentiating with respect to time yields

$$\frac{dV}{dt} = W \frac{d}{dt}(LH_m) = W \left(H_m \frac{dL}{dt} + L \frac{dH_m}{dt} \right) = M_{tot} \, . \tag{2}$$

The mean ice thickness is parameterized as (Oerlemans, 2011)

$$H_m = S(t) \frac{\alpha}{1+\nu\bar{s}} L^{1/2} . \tag{3}$$

Here $\bar{s}$ is the mean bed slope over the glacier length, and thus varies in time when the glacier length changes. S is the "surge function", making it possible to impose a surge (to be discussed later). For a non-surging glacier we simply have $S(t) = 1$. The parameter α can be interpreted a measure of the global basal resistance of the bed to ice flow and determines the mean ice thickness for a given slope and glacier length. Because of the abundant presence of soft and presumably mostly saturated sediments at the bed, the larger glaciers on Svalbard experience rather low resistance and therefore are comparatively thin. As shown later, the value of α is therefore relatively low (typically ~ 2 m$^{1/2}$ as compared to a value of ~ 3 m$^{1/2}$ for many mid-latitude glaciers, or even ~ 3.5 m$^{1/2}$ for glaciers that are (partly) cold-based, like McCall glacier in Alaska (Oerlemans, 2011). The parameter ν determines the dependence of the mean ice thickness on the mean bed slope. Based on a large number of numerical experiments with an ice flow model (Oerlemans, 2001), its dimensionless value was set to 10.

Substituting the time derivative of Eq. (2) into Eq. (3) gives

$$\frac{dV}{dt} = \frac{WH_m}{S} \left\{ L \frac{dS}{dt} + \frac{3}{2} S \frac{dL}{dt} \right\} \tag{4}$$

https://doi.org/10.5194/tc-2021-155
Preprint. Discussion started: 15 June 2021

105 Rearranging then yields the prognostic equation for L:

$$\frac{dL}{dt} = \frac{2M_{tot}}{3\,WH_m} - \frac{2}{3}\frac{1}{S}\frac{dS}{dt}\,L \tag{5}$$

We have neglected a term involving $\frac{\partial \bar{s}}{\partial L}$ because it is generally small. However, the dependence of the mean ice thickness on the mean bed slope is still retained through Eq. (3). See section 5 in Oerlemans (2011) for more discussion.

The next step is to determine the mass budget, and we first consider the surface budget. The balance rate is assumed to be a
110 linear function of altitude relative to the equilibrium-line altitude E (see the compilation in Oerlemans and Van Pelt, 2015):

$$\dot{b} = \beta(h - E)\ , \tag{6}$$

Where β is the balance gradient and E is the equilibrium-line altitude.

The total mass loss or gain of the flowband is found by integrating the balance rate over the glacier length:

$$B_s = \beta W \int_0^L [H(x) + b(x) - E]dx = \beta W\big(H_m + \bar{b} - E\big)L\ , \tag{7}$$

115 where $\bar{b}$ is the mean bed elevation of the glacier (note that this quantity as well as H_m depends on the glacier length, which in fact introduces the height - mass balance feedback).

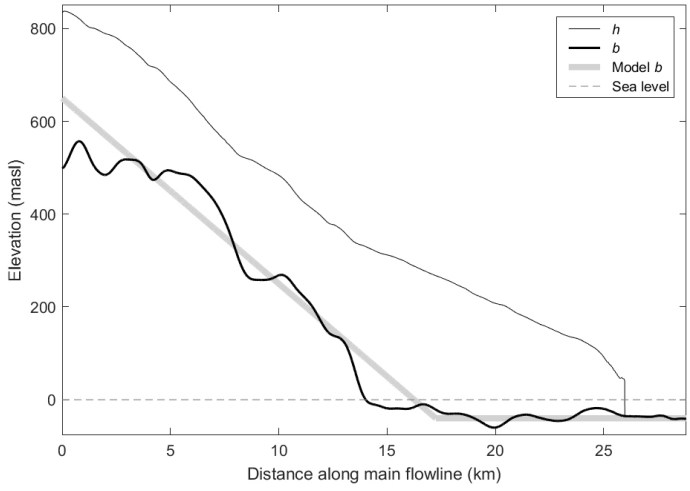

Figure 4. Cross-section along centerline profile (shown in Figure 3) of the main flow band, with band-averages of: surface
120 **topography (thin black line) from the 2009/2011 NPI DEM, bed topography from the Fürst et al (2018) reconstruction (0-12.5 km), 2015 helicopter radar measurements (12.5-25 km), and hydrographic data in the fjord (Norwegian Mapping Authority Hydrographic Service). A piecewise linear profile is fit to the bed profile for the MGM.**

2.2 Geometry

The bed topography of the main stream as defined in Figure 3 is not very well known. The bed topography of Svalbard glaciers
125 has been modelled (Fürst et al., 2018) using a balance velocity approach, overridden by observed topography where radar data are available. For Tunabreen, radar surveys were carried out by the Norwegian Polar Institute over the lower part of the glacier

https://doi.org/10.5194/tc-2021-155
Preprint. Discussion started: 15 June 2021

(Figure 3), so that the geometry of this part of the bed is reasonably well constrained; from ~16 km and downglacier, the glacier bed is below sea level, typically -40 m. The details of the upper part of the glacier bed are not dealt with; the smaller undulations in this area presumably have a limited effect on the overall dynamics of the glacier, and it is not clear how realistic all of the undulations really are. These considerations led to the choice of a simple piecewise linear bed profile (red line in Figure 4).

So we have:

$$b(x) = b_h - s_1 x \quad (0 \le x \le L_1)\,, \tag{8a}$$

$$b(x) = b_d \quad (x > L_1)\,. \tag{8b}$$

The bed profile thus drops off linearly, at rate s_1, until $x = L_1$, from where the bed height has a constant value of b_d. The parameters used here are $b_h = 650$ m; $s_1 = 0.04$; $b_d = -40$ m. It follows that $L_1 = 17250$ m.

The mean bed elevation $\bar{b}$ and mean bed slope $\bar{s}$ for given L are now easily found:

$$\bar{b} = \{(b_h - s_1 L_1/2)L_1 + b_d\,(L - L_1)\}\,/L \quad (L > L_1)\,, \tag{9a}$$

$$\bar{b} = (b_h - s_1 L/2) \quad (L \le L_1)\,. \tag{9b}$$

$$\bar{s} = (b_h - b_d/L \quad (L > L_1)\,, \tag{10a}$$

$$\bar{s} = s_1 \quad (L \le L_1)\,. \tag{10b}$$

With these expressions the mean ice thickness as well as the surface mass budget of the main stream can be calculated for any value of L.

The tributary basins have a fixed geometry. The mass budget of an individual basin is then given by

$$M_i = \beta \iint_{A_i} (h - E)dA = \beta A_i\left(\bar{h}_i - E\right)\,, \tag{11}$$

Where A_i is the area and $\bar{h}_i$ is the mean surface elevation of basin i (determined from a digital elevation model). When $M_i > 0$, the mass is added to the budget of the main stream. When $M_i \le 0$, there is no coupling between basin and main stream. For the present geometry of the basins this happens when $E > 853, 747$ and 663 m a.s.l. for basins 1, 2 and 3, respectively.

2.3 Calving rate

In the earlier studies with MGMs (Hansbreen, Oerlemans et al. 2011; Monacobreen, Oerlemans, 2018), the calving rate was assumed to be proportional to the water depth. However, recent field and remote sensing studies show that the dominant control on calving at many Svalbard tidewater glaciers is undercutting of the submerged ice front by melting (Petlicki et al., 2015; Luckman et al., 2015; How et al., 2019). An appropriate calving law would thus have water temperature of the fjord as a major parameter. However, water temperatures for the past 120 years are not available for Tempelfjorden, and therefore in the standard set-up of the model the calving rate has been taken constant and equal to the observed mean value for the period 2012-2019, namely 270 m a^{-1}. This may overestimate calving rates further back in time, but in any case we will investigate later how different calving rate affect the length of Tunabreen.

To make a smooth transition from a tidewater glacier to a land-based glacier possible, the calving flux should go smoothly to zero when the water depth approaches zero. We deal with this by writing the calving flux as

$$F = -K\,W H_f \tan^{-1}(d/3)\,, \tag{12}$$

where K is the calving rate, W is the glacier width, H_f is the ice thickness at the glacier front, and d is the water depth at the front (in m).

https://doi.org/10.5194/tc-2021-155
Preprint. Discussion started: 15 June 2021

The thickness at the glacier front is not explicitly calculated and therefore has to be parameterized. As for the studies of Hansbreen and Monacobreen referred to above, the following parameterization is used:

$$H_f = \max\{\kappa H_m; \delta\}\,. \tag{13}$$

Here δ is the ratio of water density to ice density, and κ is a constant giving the ratio of the frontal ice thickness to the mean ice thickness. For the current geometry of Tunabreen, $\kappa \cong 0.3$. So according to Eq. (13) the ice thickness can never be less than the critical thickness for flotation. The use of Eqs. (12) and (13) allows the model glacier to undergo a smooth transition between a land-based terminus and a calving front, which is a prerequisite for long-term simulations in which a model glacier should have the possibility to grow from zero volume to a long calving glacier, and backwards.

2.4 Imposing surges

In the MGM surges are not internally generated but have to be prescribed. For a discussion on surging mechanisms the reader is referred to, among others, Sund et al. (2009), Mansell et al. (2012), and Benn et al. (2019). Including surges is potentially important, because they affect the mass budget and thus may exert an influence on the long-term evolution of a glacier. When a glacier surges and its front advances, the mean surface elevation decreases and the ablation zone expands. In the MGM a surge is imposed through the function $S(t)$ in Eq. (3). A fast decrease in S implies a smaller ice thickness, and to fulfil mass conservation the glacier length has to increase. So the surge is in fact modelled as a sudden reduction in the mean basal resistance, without specifying its cause, where it is initiated or how it propagates.
In the model the surge function is prescribed as (Oerlemans, 2011):

$$S(t) = 1 - S_0(t - t_0)e^{-(t-t_0)/t_s}\,. \tag{14}$$

The surge starts at $t = t_0$. Two additional parameters, S_0 and t_s, determine the amplitude and the characteristic time scale of the surge. In the earlier studies of Abrahamsenbreen and Monacobreen, periodic surging was imposed, with fixed values of S_0 and t_s according to the observed single surge of these glaciers. However, in the case of Tunabreen four surges of different amplitude and duration have been observed, which are included in the model by using different surge parameters. This allows a closer match between observed and simulated glacier length.

2.5 Climate forcing

Information on the climate history of Svalbard is mainly based on geomorphological and geological studies (e.g. CAPE, 2006; Bradley, 2016; Axford et al., 2017; Farnsworth et al., 2020). The general picture emerging from these studies is that of a warmer mid-Holocene climate with much reduced glacier extent over Svalbard, with gradual cooling afterwards. This cooling of 1 to 3 degrees is normally interpreted as a direct insolation effect (changing orbital parameters reducing summer radiation). Most glaciers on Svalbard reached maximum stands during the local Little Ice Age, between 1850 and 1900 (e.g. Martin-Moreno et al., 2017). Significant warming started around 1900 (Divine et al., 2011) and continues until today, but with some interruptions, notably between 1950 and 1980. On Svalbard the relation between the ELA and meteorological parameters is perhaps more complicated than for mid-latitude conditions, partly because refreezing plays a larger role. We have considered results from a detailed energy-balance model of Svalbard mass balance (Van Pelt et al., 2019) to derive model ELA values for Tunabreen, for the period 1957-2020. However, to have a useful ELA history to simulate observed glacier length, this reconstruction has to be extended backwards to at least 1900. We tried to do this by means of a reduced major axis regression on the modelled ELA to meteorological parameters observed at Longyearbyen (Nordli et al., 2020; Førland et al., 2011, with

https://doi.org/10.5194/tc-2021-155
Preprint. Discussion started: 15 June 2021


The Cryosphere Discussions
Open Access
EGU

updates). The correlation with summer temperature appears to be significant (coefficient 0.46), but in the end explains only 25% of the ELA variability. In spite of this, we reconstructed the ELA history back to 1900 (referred to later as ELA_{LYR}). Some test calculations with the resulting forcing function were not satisfactory (this will be shown and discussed later), and therefore it was decided to use for the reference experiment a forcing function of a smooth and simple form, in line with the statement in the beginning of this section. The forcing is written as

$$E(t) = E_0 + c_1(t - 1900)^2 - c_2 e^{-((t-1975)/30)^2}. \quad (15)$$

According to Eq. (15), the equilibrium line rises quadratically in time. On this rise a depression of Gaussian shape is superposed, centred around the year 1975 and having a characteristic window of 30 years. In the simulation of the observed length record, the parameters E_0, c_1 and c_2 are determined in such a way that the best possible match between observed and simulated glacier length is obtained. So in effect, the climate forcing is reconstructed by inverse modelling on the glacier length observations.

3 Basic experiments on the sensitivity of Tunabreen to climate change

Before discussing simulations with the time-dependent climatic forcing described in section 2.5, it is useful to obtain a feeling for the sensitivity of glacier length to environmental parameters like the ELA and the calving rate. We can obtain insight into climate sensitivity and response times by doing this in numerical experiments with stepwise forcing imposed on a steady state. First of all the value of α in eq. (3) was obtained by matching the simulated and observed mean ice thickness (for the profile shown in Figure 4), yielding $\alpha = 1.96\ \mathrm{m}^{1/2}$. With $E = 491$ m and K = 270 m a^{-1}, the model now produces a steady-state glacier with a length that corresponds to the situation around 1920 ($L \approx 25.8$ km). In this case the net balance of the main stream is - 0.14 m w.e. a^{-1}, of the tributaries + 1.30 m w.e. a^{-1}, and from calving -1.16 m w.e. a^{-1}, the latter obtained by dividing calving flux by glacier area for a good comparison. So although the main stream also has an accumulation area (Figure 3), its mean surface balance is negative and the influx from the tributaries is essential to maintain the long glacier tongue of Tunabreen.

In Figure 5 glacier length is shown for different perturbations of the ELA. All integrations start at t = 0, and the perturbation in the forcing is applied at t = 1500 a (to make sure that the initial state represents a steady state). For a 25 m rise of the equilibrium line the glacier would become about 4 km shorter, but it takes a long time to approach a steady state (~ 400 years). The large climate sensitivity (defined as $\partial L/\partial E$) and long timescale is a consequence of the very small mean bed (and surface) slope (Oerlemans, 2001, 2011). For larger perturbations of the ELA (+50 m, +100 m) the sensitivity becomes less and the response time shorter (typically ~100 a for the case with $\Delta E = +100$ m). This is related to the position of the glacier snout. When the glacier snout is still calving but on the upward sloping part of the bed (Figure 4), the dependence of the calving flux on the water depth makes the glacier more stable (a smaller change in L is needed to achieve the necessary change in the mass budget to acquire a new equilibrium state). The height – mass balance feedback becomes particularly effective for negative values of ΔE. Because the calving rate is constant there is no way for the model glacier to stabilize. In reality the advance would come to a halt because the glacier front will eventually encounter deeper water and higher water temperatures.

The red curves in Figure 5 shows the response of the glacier to changes in the calving rate K. For a 50 % larger calving rate, i.e. 405 m a^{-1}, the response of the glacier is quite comparable to the case with $\Delta E = +50$ m. For a 25% decrease in the calving rate, the glacier grows slowly, but steadily.

https://doi.org/10.5194/tc-2021-155
Preprint. Discussion started: 15 June 2021

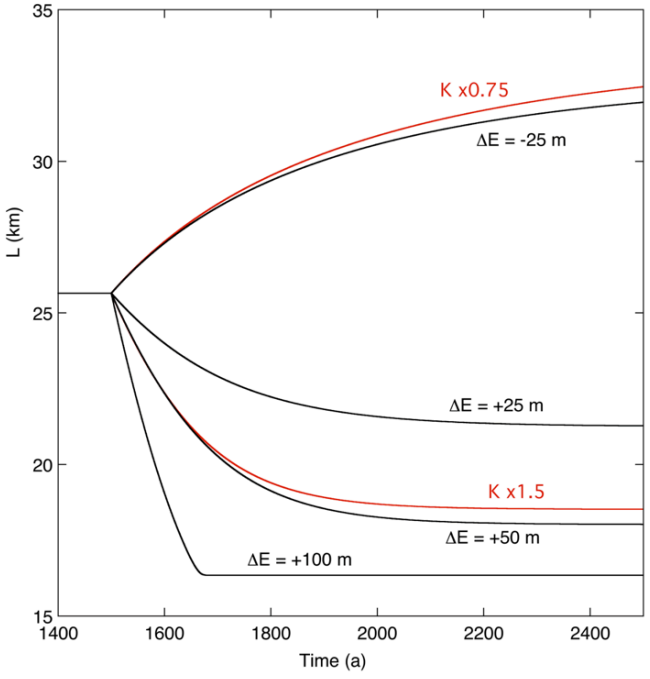

Figure 5. Evolution of glacier length for different perturbations of the ELA (ΔE), and for different values of the calving rate K.

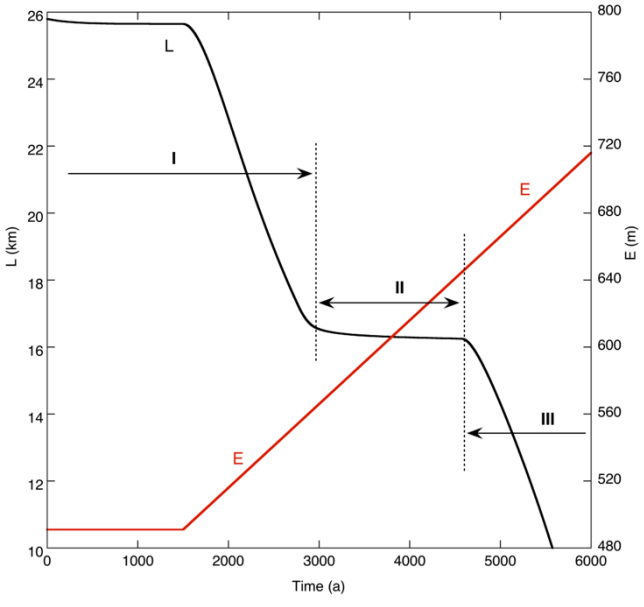

Figure 6. Glacier length L for a very slowly increasing ELA (E). Three regimes are identified (I, II, III) for which the sensitivity of glacier length to the ELA ($\partial L/\partial E$) differs significantly.

https://doi.org/10.5194/tc-2021-155
Preprint. Discussion started: 15 June 2021

245 The apparent differences in the sensitivity for smaller and larger perturbations of the ELA call for a further numerical experiment in which this is explored. One way to approach this is to do a long integration with very 'slow' forcing (here slow means that the glacier is always close to an equilibrium state). Figure 6 shows the result of an integration in which the ELA increases at a rate of 0.05 m a^{-1}. Evidently, with respect to the climate sensitivity $\partial L/\partial E$ (dimensionless), three regimes can be distinguished. In regime I the glacier front is calving and located on the part of the bed with constant water depth. The mean
250 climate sensitivity in this regime is $\partial L/\partial E \approx 150$. As noted before, this very large value is a direct consequence of the small mean bed slope (strong height - mass balance feedback). In regime II the glacier front is on the part of the bed where the water depth decreases when going inland. When the glacier becomes shorter to adapt to the increasing ELA, the calving rate decreases strongly (according to Eq. (12)). A very small change in L is therefore sufficient to restore equilibrium, and consequently the climate sensitivity is small ($\partial L/\partial E \approx 5$). In regime III the glacier has become a land-based glacier. The
255 combined effect of a larger mean bed slope and the absence of calving results in a climate sensitivity comparable to that for regime I (now $\partial L/\partial E \approx 140$). This calculation thus illustrates once more how important geometric factors are when considering the response of individual glaciers to climate change.

4 Simulating the evolution of Tunabreen during the past 100 years

We now turn to simulation of the observed length record. The best possible result for optimal values of the surge parameters
260 (t_0, S_0, t_s) and climatic parameters (E_0, c_1, c_2) is shown in Figure 7. The value of E_0 was set to a value that makes the simulated glacier length in 1924 equal to the observed value ($E_0 = 490$ m a.s.l.). The surge amplitudes have been chosen such that the advance during the surge approximately matches the observed length change.

During the 1924 surge, which has the largest amplitude ($\Delta L \approx 3$ km), the associated maximum reduction in the mean ice thickness (and surface elevation) is about 25 m. Although the calving rate is constant, the calving flux decreases slightly
265 because the frontal ice thickness is somewhat smaller. Altogether, at the end of the surge the net mass budget perturbation of the main stream is about -0.24 m w.e. a^{-1} and of the entire glacier about -0.18 m w.e. a^{-1}. It should be noted that there are two effects leading to a negative balance perturbation: (i) the lowering of the glacier surface, and (ii) the extension of the ablation zone. Together with the climatic forcing this affects the retreat of the glacier front after the surge.

For the 1966-1971 surge the simulated retreat is somewhat too fast. However, increasing the surge parameter t_s does not help
270 because it leads to a glacier length that is too large when the next surge starts. The last surge comes fast and has a small amplitude, but it was possible to choose the surge parameters in such a way that the 2020 observed length is reproduced. The dotted line in Figure 7 shows the result for a run without surging. In this case the glacier length stays close to the minimum values after each surge except for the large part. The 2016 surge comes so fast after the previous surge that the glacier has no time to adjust its length to the higher ELA.

275 The result of Figure 7 has been obtained with the following parameters of the ELA history: $E_0 = 490$ m a.s.l., $c_1 = 0.01$ m a^{-2}, $c_2 = 40$ m. Changing these parameters leads to a larger difference between observed and simulated glacier length. This cannot be compensated by adjusting the surge parameters, i.e. the parameter sets (t_0, S_0, t_s) and (E_0, c_1, c_2) play fairly independent roles in the model. The ELA history that delivers the best simulation is therefore well determined and reveals that a 100 m increase in the ELA over the past 50 years is sufficient to explain the behaviour of Tunabreen. At this point it is
280 interesting to return to the ELA reconstruction based on energy-balance modelling and the Longyearbyen meteorological record as discussed in section 2.5 (ELA_{LYR}).

https://doi.org/10.5194/tc-2021-155
Preprint. Discussion started: 15 June 2021

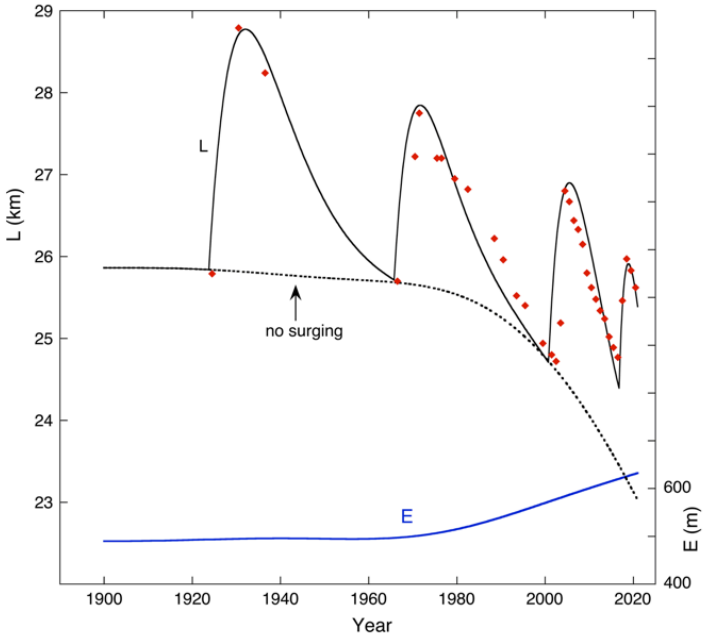

Figure 7. Simulation of glacier length *L* achieved after optimization of the model parameters. Observations are indicated by red dots. The blue line shows the optimal ELA forcing (scale at right). Glacier length simulated for a case without surging is shown by the dotted line.

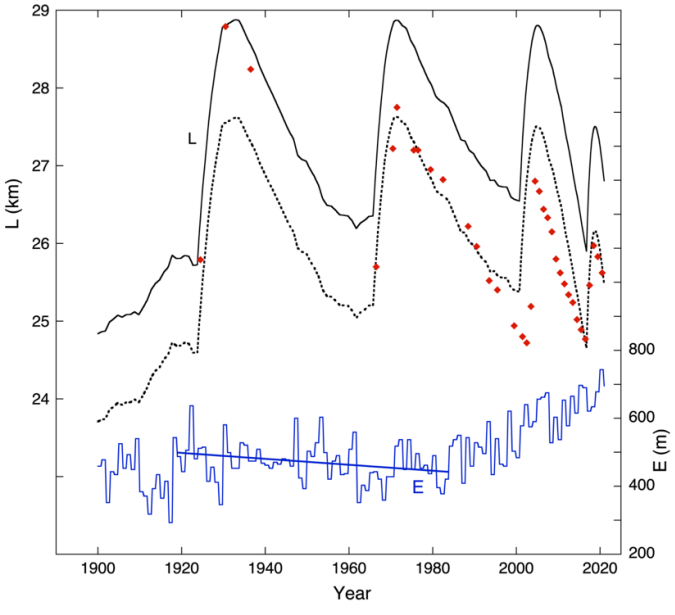

Figure 8. Simulation of glacier length *L* with ELA_{LYR} as climate forcing (scale at right). Observations are indicated by red dots. The simulation shown by the solid line is tuned to the first observed glacier length (1926), the dotted line is tuned to the last observed glacier length (2020).

https://doi.org/10.5194/tc-2021-155
Preprint. Discussion started: 15 June 2021

In Figure 8 computed glacier length is shown for the ELA_{Longy} forcing. Two simulations are shown: one in which the first data point (1926) is matched with the observed length, one in which the last data point (2020) is matched. The corresponding value of E_0 are 495 and 501 m.

None of the simulations is good, and adjusting the surge parameters does not give an improvement. The reason for the discrepancy between observed and simulated glacier length is the small but significant decline of the ELA during the period 1920 – 1980. When the equilibrium line starts to rise around 1985, the response of the glacier is too slow to catch up with the observed retreat over the last hundred years. It thus appears that the value of ELA_{LYR} as a climate proxy for Tunabreen is limited.

5 The future evolution of Tunabreen

Having calibrated the model with observations over the past hundred years, we now consider future climate change scenarios and see how Tunabreen might change in the coming hundred years. Rather than applying the output from regional climate model simulations with all their uncertainties, we prefer a simple approach in which the equilibrium line rises at a constant rate after the year 2020.

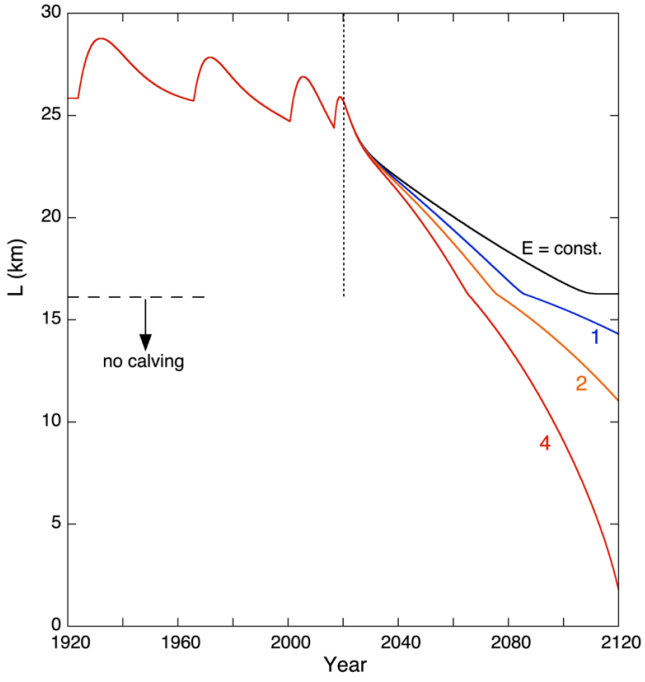

Figure 9. Glacier length *L* for different climate change experiments. The black curve refers to a calculation in which *E* is kept constant at its 2000 - 2019 mean value. The colour labels refer to the imposed constant rate of change of *E* per year from 2020 onwards.

In Figure 9 some results of climate change experiments for the next hundred years are summarized. In the reference run the ELA is kept constant at the 2020 value from the reconstruction, namely 630 m a.s.l. In this case the glacier retreats during the next hundred years at an almost linear rate of ~80 m a^{-1}, which illustrates by how much the current glacier stand is out of

https://doi.org/10.5194/tc-2021-155
Preprint. Discussion started: 15 June 2021

equilibrium with the present climate. Around the year 2110 a new steady state would be reached, with a glacier length of 16.2 km and no calving anymore.

For the intermediate climate warming scenario (the equilibrium line then rises by 2 m a^{-1}), Tunabreen would retreat by about 13 km over the next hundred years. During the retreat the net balance would steadily decrease to about -1.7 m w.e. a^{-1} m^{-1}, i.e. the glacier is getting more and more out of balance. In the year 2037 basin 3 would no longer deliver mass to the main stream, for basin 2 this happens in the year 2078.

For the case of a 4 m a^{-1} rise in the equilibrium line, the retreat is obviously much stronger and by the year 2120 Tunabreen has almost disappeared. In the year 2087, $E = 900$ m a.s.l. and virtually the entire glacier is below the equilibrium line.

It can be seen in all the simulations that the retreat slows down somewhat when the glacier becomes land-based and calving stops (at $x = 16.2$ km, dashed line in Figure 9).

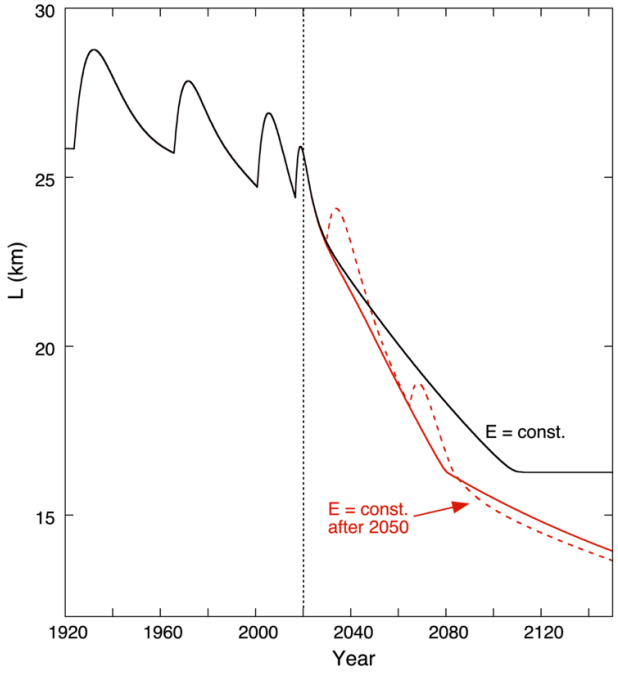

Figure 10. Glacier length *L* for the 'Paris run' (constant ELA after 2050), shown in red. The black curve refers to the calculation in which *E* is kept constant at its 2020 reconstructed value (as in Figure 9). The dashed curve represents the 'Paris run' with two surges imposed, starting in 2030 and 2065.

In Figure 10 a calculation is shown for an optimistic climate change scenario, in which the equilibrium line rises by 2 m a^{-1} until the year 2050 and remains constant afterwards (we refer to this calculation as the 'Paris run'). We show the result until the year 2150, to see if by this time the glacier would have reached a new steady state. Obviously, this is not the case, although the rate of retreat slows down. This case clearly illustrates that it takes a long time before limiting climate warming has a significant effect on the retreat of large glaciers.

To further illustrate the interaction between climate change and the mass budget of Tunabreen, we show in Figure 11 the various mass balance components as a function of time for the 'Paris run' (without additional surges). All terms in the mass

https://doi.org/10.5194/tc-2021-155
Preprint. Discussion started: 15 June 2021

budget equation have been converted to specific balance rate for an easy comparison, e.g. the calving flux has been divided by the glacier area. First of all, as noted before, the balance of the main stream (*bstream*) is always negative and the glacier lives on the contributions from the tributaries (*btrib*). After 2050 the specific contribution from the tributaries increases slightly, in spite of the fact that they have a fixed geometry and the ELA is constant. The increase occurs because the area of the main stream is decreasing and thereby the relative contribution of the tributaries is increasing. The calving rate (*bcal*) is little affected until the front comes into shallow water and then retreats on land.

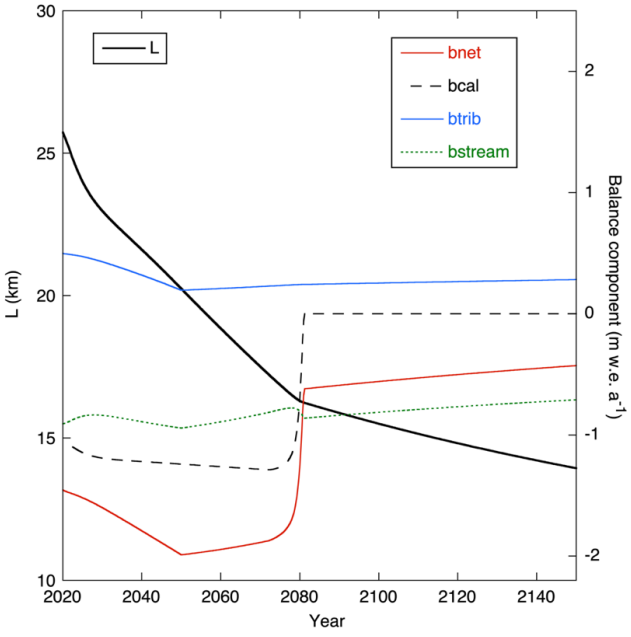

Figure 11. Glacier length (solid black line, scale at left) and mass balance components (scale at right) for the 'Paris run'.

5 Discussion

Tunabreen is a special glacier because of its complex surging behaviour, which poses a real challenge for a modelling study. The MGM, based on the view that the evolution of a glacier is first of all determined by the exchange of mass with its surroundings, offers a relatively simple tool to study the response of Tunabreen to changing environmental conditions. The application is straightforward and requires as geometric input only a topographic map and a schematic bed profile along the main flow band. Although in the end one would like to repeat the simulations presented here with a comprehensive glacier flow model with spatial resolution, it will not be an easy task to prepare the necessary input fields and get the calving and surging at the right place and time !

As has been found for other larger glaciers in Svalbard, Tunabreen appears to be very sensitive to climate change. The common factor is the small surface slope, also when considered in a global perspective. From a purely geometric argument, $\partial L/\partial E \approx -2/\bar{s}$ (Oerlemans, 2001). The mean slope of Tunabreen is 0.031, comparable to that of many other glaciers in Svalbard like e.g. Monacobreen (0.025), Kongsvegen (0.032), Kronebreen (0.025). A characteristic value of $\partial L/\partial E$ therefore is -65, i.e. a 100 m rise of the equilibrium line implies a glacier retreat over 6.5 km (when a steady state would be reached). For larger mid-latitude mountain glaciers values of $\partial L/\partial E$ are in the range of -10 to -30, while for long glaciers in Alaska and

https://doi.org/10.5194/tc-2021-155
Preprint. Discussion started: 15 June 2021

Patagonia typically in the range of -30 to -60. Although other factors than mean slope play a role, it is fair to conclude that the larger glaciers on Svalbard are the most sensitive in the world. This is in line with the idea that during the mid-Holocene Climatic Optimum the degree of glacierization in Svalbard was considerably smaller than today (e.g. Fjeldskaar et al., 2017). Our numerical experiments suggest that typical fluctuations in calving rates and equilibrium line altitudes have comparable effects on the evolution of Tunabreen. A 50 % increase in the calving rate has the same effect as a 50 m increase of the ELA (Figure 6). It is conceivable that in a warming climate with increasing ocean temperatures, calving rates will become larger. This implies that the glacier retreat curves shown in Figure 9 represent conservative estimates. However, further studies on the relation between ocean temperatures and calving rates on multi-annual time scale are needed to make a meaningful estimate of how calving might enhance the retreat of Tunabreen in the near future.

We did not find a significant impact of surging on the evolution of Tunabreen. Although a surge initiates a negative perturbation of the mass budget for some years and reduces the glacier volume slightly, apparently this has no lasting effect. The same conclusion was reached in earlier studies of Abrahamsenbreen (Oerlemans and Van Pelt, 2015) and Monacobreen (Oerlemans, 2018), and it probably applies to most long glaciers on Svalbard. However, with respect to ice caps that have surging parts (like Austfonna), the situation may be different.

Author contribution

JO developed the model code and performed the simulations. JK analysed and evaluated data on bedrock topography and glacier length. AL derived and compiled data on calving rates. JO prepared the manuscript with contributions from all co-authors.

References

Axford, Y., Levy, L. B., Kelly, M. A., Francis, D. R., Hall, B. L., Langdon, P.G., and Lowell, T. V.: Timing and magnitude of early to middle Holocene warming in East Greenland inferred from chironmids, Boreas, doi.org/10.1111/bor.12247, 2017.

Benn, D. I., Fowler, A. C., Hewitt, I., Sevestre, H.: A general theory of glacier surges, J. Glaciol., 1–16, https://doi.org/10.1017/jog.2019.62, 2019.

Bradley, R. S.: Holocene climate change in Arctic Canada and Greenland, Qua. Sci. Rev., doi.org/10.1016/j.quascirev.2016.02.010, 2006.

CAPE-Last Interglacial Project Members: Last Interglacial Arctic warmth confirms polar amplification of climate change. Quat. Sci. Rev., 25, 1383-1400, doi.org/10.1016/j.quascirev.2006.01.033, 2006.

Divine, D., Isaksson, E., Martma, T., Meijer, H. A. J., Moore, J., Pohjola, V., Van de Wal, R. S. W. ,and Godtliebsen, F.: Thousand years of winter surface air temperature variations in Svalbard and northern Norway reconstructed from ice- core data, Polar Res., 30 (1), 7379, DOI: 10.3402/polar.v30i0.7379, 2011

Farnsworth, W. R., Allaart, L., Ingólfsson, Ó., Alexanderson, H., Forwick, M., Noormets, R., Retelle, M. and Schomacker, A.: Holocene glacial history of Svalbard: Status, perspectives and challenges, Earth-Science Rev., 208, https://doi.org/10.1016/j.earscirev.2020.103249, 2020

Fjeldskaar, W., Bondevik, S., and Amantov, A.: Glaciers on Svalbard survived the Holocene thermal optimum, Quat. Sci. Rev., 119, 18-29, doi.org/10.1016/j.quascirev.2018.09.003, 2017.

395 Flink, A. E., Noormets, R., Kirchner, N., Benn, D. I., Lovell, H.: The evolution of a submarine landform record following recent and multiple surges of Tunabreen glacier, Svalbard, Quat. Sci. Rev., 108, 37-50, doi.org/10.1016/j.quascirev.2014.11.006, 2015.

Fowler, A. C., Murray, T., Ng, F. S. L.: Thermally controlled glacier surges. J. Glaciol., 47, 527–538, 2001.

Førland, E. J., Benestad, R., Hanssen-Baur, I., Haugen, J. E. and Skaugen, T. E.: Temperature and precipitation development
400 at Svalbard 1900-2100, Adv. Meteorol., 2011, doi: 10.1155/2011/893790, 2011.

Fürst, J. J., and 25 others: The ice free topography of Svalbard, Geophys. Res. L., 45, 11760-11769, https://doi.org/10.1029/2018GL079734, 2018.

How, P., Schild, K. M., Benn, D. I., Noormets, R., Kirchner, N., Luckman, A., Vallot, D., Hulton, N. R., Borstad, C.: Calving controlled by melt-under-cutting: detailed calving styles revealed through time-lapse observations, Ann. Glaciol., 60 (78), 20-
405 31, doi:10.1017/aog.2018.28, 2019.

Luckman, E., Benn, D. I., Cottier, F., Bevan, S., Nilsen, F., Inall, N.: Calving rates at tidewater glaciers vary strongly with ocean temperature, Nature Communications, 6 (1), 1-7, doi: 10.1038/ncomms9566 |www.nature.com/naturecommunications, 2015.

Mansell, D., Luckman, A. and Murray, T.: Dynamics of tidewater surge-type glaciers in northwest Svalbard, J. Glaciol., 58,
410 110-118, doi: 10.3189/2012JoG11J058, 2012.

Martín-Moreno, A., Alvarez, F. A. and Hagen J. O.: 'Little Ice Age' glacier extent and subsequent retreat in Svalbard archipelago, The Holocene, 27 (9), 1379-1390, doi.or/10.1177/0959683617693904, 2017.

Nordli, Ø., Wyszyński, P., Gjelten, H. M., Isaksen, K., Łupikasza, E., Niedźwiedź, T., and Przybylak, R.: Revisiting the extended Svalbard Airport monthly temperature series, and the compiled corresponding daily series 1898–2018, Polar
415 Res., 39. doi.org/10.33265/polar.v39.3614, 2020

Norwegian Polar Institute: Terrengmodell Svalbard (S0 Terrengmodell) [Data set]. Norwegian Polar Institute. doi:10.21334/npolar.2014.dce53a47, 2014

Oerlemans, J.: Glaciers and Climate Change. A.A. Balkema Publishers, 148 pp. ISBN 9026518137, 2001.

Oerlemans, J.: Minimal Glacier Models, Second edition, Igitur, Utrecht University, ISBN 978-90-6701-022-1, 2011.

420 Oerlemans, J.: Modelling the late Holocene and future evolution of Monacobreen, northern Spitsbergen, The Cryosphere, 12, 3001-3015, doi.org/10.5194/tc-12-3001-2018, 2018.

Oerlemans, J. and Van Pelt, W. J. J.: A model study of Abrahamsenbreen, a surging glacier in northern Spitsbergen, The Cryosphere 9, 767-779, doi: 10.5194/tc-9-767-2015, 2015.

Petlicki, M., Cieply, M., Jania, J. A., Prominska, A., Kinnard, C.: Calving of a tidewater glacier driven by melting at the
425 waterline, J. Glaciol., 61 (229), 851-863, doi: 10.3189/2015JoG15J062, 2015.

Sund, M., Eiken, T., Hagen, J. O., Kääb, A.: Svalbard surge dynamics derived from geometric changes, Ann. Glaciol., 50 (52), 50-61, 2009.

https://doi.org/10.5194/tc-2021-155
Preprint. Discussion started: 15 June 2021

Van Pelt, W. J. J., Oerlemans, J., Reijmer, C. H., Pohjola, V. A., Petterson, R., and Van Angelen, J. H.: Simulating melt, runoff and refreezing on Nordenskiöldbreen, Svalbard, using a coupled snow and energy balance model, The Cryosphere, 6, 347-360, doi: 10.3189/2012/JoG11J217, 2012.

Van Pelt, W., Pohjola, V., Petterson, R., Marchenko, S., Kohler, J., Luks, B., Hagen, J. O., Schuler, T. V., Dunse, T., Noël, B., Reijmer, C.: A long-term dataset of climtic mass balace, snow conditions, and runoff in Svalbard (1957-2018), The Cryosphere, 13 (9), 2259-2280, https://doi.org/10.5194/tc-13-2259-2019, 2019.

Welty, E., Zemp, M., Navarro, F., Huss, M., Fürst, J. J., Gärtner-Roer, I., Landmann, J., Machguth, H., Naegeli, K., Andreassen, L. M., Farinotti, D., Li, H., and GlaThiDa Contributors: Worldwide version-controlled database of glacier thickness observations, Earth Syst. Sci. Data, 12, 3039–3055, https://doi.org/10.5194/essd-12-3039-2020, 2020.